

THE POTENTIAL BARRIER DETERMINATION OF STRONTIUM DOPED TITANIUM OXIDE VARISTOR

T. Delbrücke¹, I. Schmidt¹, J. R. Jurado^{1,2,3}, S. Cava¹, V. C. Sousa¹

¹Laboratory of Biomaterials & Advanced Ceramics, Engineering Materials
Department, Federal University of Rio Grande do Sul, 91501-970,

Porto Alegre, RS, Brazil

²Postgraduate Program in Science and Materials Engineering, Technology
Development Center, Federal University of Pelotas, 96010-900,

Pelotas, RS, Brazil

³Glass Department, Institute of Glass and Ceramic, 28049, Madrid, Spain

tiagodt@gmail.com

ABSTRACT

In polycrystalline semiconductors, nonlinear charge transport is governed by the grain boundary electronic structure and described through a double Schottky barrier model. The addition of different dopants affects the densification and electrical properties of TiO₂-based varistor ceramics. The potential barrier is examined when doped with small quantities (0.5-2 at.%) of strontium oxide, and this results will be related with nonlinear current (I) and voltage (V) characteristics of titanium dioxide. This paper discusses the electrical properties of such an SrO doped TiO₂ system, and demonstrates that some combinations produce electrical properties suitable for use as low voltage varistors. The high value of the nonlinear coefficient (α) (6.6), the breakdown electric field (E_b) (328 V/cm) and the leakage current (I_r) (0.22 mA/cm²) obtained in a system newly doped with SrO, are all adequate properties for application in low voltage varistors.

Keywords: electrical properties, potential barrier, SrO, TiO₂, varistors

INTRODUCTION

Titanium dioxide is an oxide of a technology that has potential applicability as a low-voltage varistor. TiO_2 is an *n*-type semiconductor, where electrons of the 3d orbitals are conducting and have low mobility^(1,2).

The TiO_2 -based varistor has attracted much interest in recent years. *Yan and Rhodes* first reported that (Nb, Ba)-doped TiO_2 ceramics have useful nonlinear properties with nonlinear coefficient of $\alpha = 3 - 4$ ⁽³⁾. In recent studies *Sousa et al.* has studied various dopants (CoO, Ta_2O_5 , Pr_2O_3 , MnO_2 and Cr_2O_3) in TiO_2 system and obtained a maximum nonlinear coefficient of $\alpha = 8.23$ with the system TiO_2 - Ta_2O_5 - MnO_2 - Cr_2O_3 ^(4,5). The study of a TiO_2 -SrO binary varistor system has been little studied and little data are found in the literature on the addition of SrO in TiO_2 . *Wang et al.*⁽⁶⁾ studied the effects of Sr on the microstructure and electrical properties of (Co, Ta)-doped SnO_2 varistors and succeeded in adding Sr, improving the electrical and microstructural properties of the system under study.

The main parameter of a varistor is the nonlinear coefficient α , other important parameters are the breakdown electrical field E_b , leakage current I_r and resistivity. An ideal varistor features high capacity of energy absorption, high value of coefficient of nonlinearity, low leakage current, high breakdown voltage and fast response against voltage transients. The ideal varistor must possess a potential barrier that prevents the passage of electrons between grains up to a certain predetermined electric field is reached, where up on the potential barrier is overcome by all electrons^(4,7).

Electrical behavior allow us to understand the formation of the potential barrier and knowing you have a strong influence on the electrical properties of varistors can know better what are the processing steps that influence their formation and therefore get varistors with higher efficiency⁽⁹⁾. In polycrystalline semiconductors, nonlinear charge transport is governed by the grain boundary electronic structure^(9,10), and described through a double Schottky barrier model⁽¹¹⁻¹³⁾.

This work proposes to investigate how the dopant SrO can modify the electrical parameters through the potential barriers and to observe the TiO_2 -based system microstructure to correlate nonohmic properties.

MATERIALS AND METHODS

The powders were obtained by a conventional oxide mixing method using the following compounds: TiO₂ (Vetec) and SrO (Aldrich). The molar compositions studied were: (TS1) 99.50% TiO₂ + 0.50% SrO (TS2) 99.00% TiO₂ + 1.00% SrO (TS3) 89.50% TiO₂ + 1.50% SrO (TS4) 88.00% TiO₂ + 2.00% SrO. The material was blended for 4 h in a ball mill, using distilled water as the dispersion medium and alcohol polyvinyl (PVAI) as ligant. After homogenization, each blend was oven dried at 110°C for 12 hours, and then forced to pass through a 200-mesh sieve (with 74 μ openings). The powders thus obtained were uniaxially pressed at 150 MPa into tablets (10 mm diameter by 1.5 mm thickness). These tablets were sintered in a MAITEC furnace at 1300-1400°C for 1 hour with a heating rate of 5°C/min and then cooled to room temperature at cooling rate of 5°C/min. The phases were identified by X-ray diffraction (XRD), using a PHILIPS X'pert MPD diffractometer. The density of the tablets was measured by the Archimedes method according to the respective international standard (ISO18754).

For electrically characterisation, disc pellets were metallized by depositing a silver ink coating on to both side of their surfaces. By analyzing their α , E_b and I_r data obtained varistor electrical transport properties. The α value was calculated from the characteristic curve of (J) as a function of the (E), and it was tested with a high voltage source (KEITHELEY, model 237), using a linear regression of the $J \times E$ curve on a logarithmic scale to determine the value of coefficient α scale starting from 1 mA/cm². The determination of the potential barrier was made by analysing impedance spectroscopy (EIS) using temperature range of 25-400°C. For this purpose a potentiostat PGSTAT, model 302N was used. The values of activation energy (E_a) were calculated by the Arrhenius Equation (A). The donor concentration (N_d) was determined using the Equation (B). On the other hand, the density of the N_{IS} states at the interface between the TiO₂ grains was estimated based on the *Mukae et al.*⁽¹⁴⁾ the following expression in Equation (C). Using the charge electroneutrality condition ($N_{IS}/N_d = 2\omega$), one can determine the width of the potential barrier (ω).

$$\ln R = \ln_0 + \frac{E_a}{K} \cdot \frac{1}{T} \quad (A)$$

$$N_d = \frac{2p}{s^2 \cdot q \cdot \epsilon_r \cdot \epsilon_0 \cdot B} \quad (B)$$

$$N_{IS} = \left(\frac{2N_d \cdot \epsilon_r \cdot \epsilon_0 \cdot \phi_b}{q} \right)^{1/2} \quad (C)$$

RESULTS AND DISCUSSION

Figure. 1 shows the X-ray diffraction patterns of powders of the materials sintered at 1300 and 1400°C. Each diagram shows the presence of a single phase, corresponding to the rutile JCPDS 01-073-1232 crystalline phase at both temperatures. From these results, it can be started that amount of SrO used does not affect the rutile formation and it was free of any secondary phase in the final sintering material.

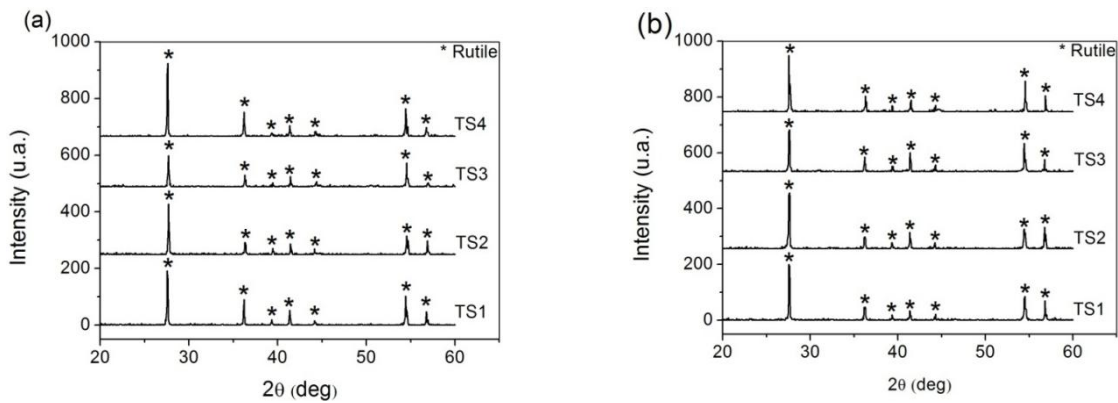


Figure 1. X-ray diffraction patterns of TS1, TS2, TS3 and TS4 powders sintered at: (a) 1300°C and (b) 1400°C.

Table 1 shows the variation in density of the samples with various SrO concentrations after sintering at 1300 and 1400°C.

Considering the ionic radius of Sr^{2+} (0.113 nm) are larger than that of Ti^{4+} (0.061 nm)⁽¹⁵⁾, the substitution of Ti^{4+} by Sr^{2+} , will cause TiO_2 lattice to distort⁽¹⁶⁾, according to the reaction of Equation (D):

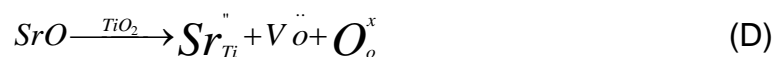


Table 1. Effect of the sintering temperature in the TS1, TS2, TS3 and TS4 systems on the apparent density (DA), apparent density (Dr) and apparent porosity (PA).

Sample	1300°C			1400°C		
	DA (g/cm ³)	Dr (%)	PA (%)	DA (g/cm ³)	Dr (%)	PA (%)
TS1	3.8	90	4.55	3.95	94	3.58
TS2	3.78	89	4.52	4	94.4	3.85
TS3	3.83	75.81	1.75	3.9	92.12	3.51
TS4	3.84	76.56	1.77	3.82	90	3.17

Figure 2a and b shows the nonlinear electrical behavior of the TiO₂-SrO arrangements with 0.5, 1.0, 1.5 and 2% percentage. The detailed data of the nonlinear coefficient, breakdown electrical field and leakage current are shown in Table 2. A SrO sample of 1% gave the best nonlinear electrical property at sintering temperatures from 1300 to 1400°C. At the sintering temperature of 1300°C on a sample with 1% SrO added, we obtained a $\alpha = 5.32$, $E_b = 440$ V/cm and $I_r = 0.46$ mA/cm². However, increasing the temperature to 1400°C while holding the 1% SrO addition constant, altered the results to $\alpha = 6.66$, $E_b = 328$ V/cm and $I_r = 0.22$ mA/cm².

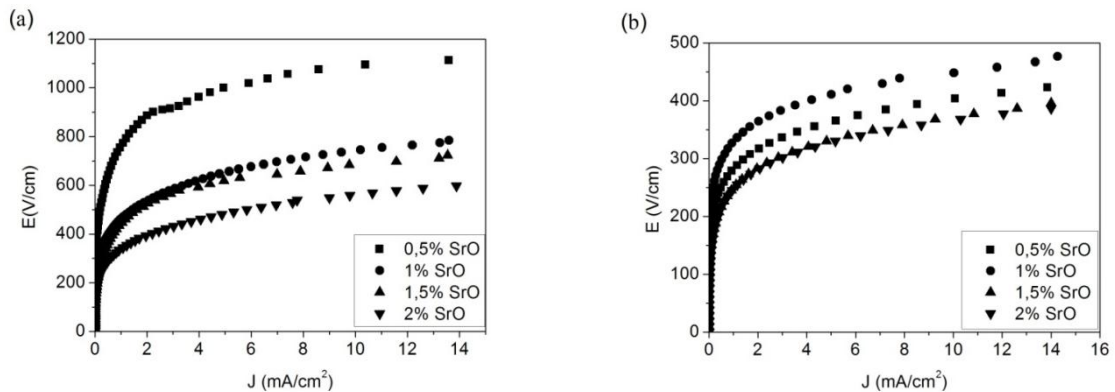


Figure 2. I - V characteristics of the TiO₂-SrO systems sintered at: (a) 1300°C and (b) 1400°C.

The nonlinear coefficient (α) tends to improve at 1400°C probably because of increased density in relation to that at 1300°C, but the increasing SrO concentration tends to decrease the α , unlike demonstrated with SnO₂⁽¹⁷⁾, it does not improve the TiO₂ densification.

Table 2. Non-linear coefficients (α), breakdown electric field (E_b) and leakage current (I_r) of the TS1, TS2, TS3 and TS4 systems sintered at 1300 and 1400°C.

Sample	1300°C			1400°C		
	α	E_b (V/cm)	I_r (mA/cm ²)	α	E_b (V/cm)	I_r (mA/cm ²)
TS1	5.39	515	1.82	6.21	281	0.26
TS2	5.32	440	2.49	6.66	328	0.22
TS3	4.6	462	1.44	5.90	250	0.19
TS4	4.17	343	1.69	5.85	248	0.33

From *EIS* results Table 3 lists several electronic of the samples sintered at 1400°C. It can be observed when the dopant concentration increases from 0.5 to 1%, there is an increase in the values of activation energy, band gap and barrier width. This increase is directly related to the value of the α value (see Table 2). However diminish the donor concentration and the states density at the grain interfaces. Results opposite are noted with increasing concentration of the dopant after 1% addition. Based on these results, it is clear that the value of nonlinear coefficient decreases at concentrations higher doping than 1% of SrO. At higher amount of donors reduce the band donor level for the electrons hopping the potential barrier, reducing the nonlinear coefficient.

The role of the absorbed oxygen in the formation of boundary barriers was addressed in the literature⁽¹⁸⁻²¹⁾. As can be seen, for each metallic ion (M^{+2}) in solid solution, an oxygen vacancy is formed, allowing for diffusion through the TiO₂ lattice and the resulting densification.

The barrier height values are lower than those observed in to ZnO-based⁽¹⁷⁾ and SnO-based⁽²²⁾ varistors, probably because not enough effective barriers were formed at the grain boundaries, a fact that explains the low nonlinear coefficient observed in these systems.

The most suitable model to explain the nonohmic behavior of nonlinear semiconductor ceramics is based on the presence of an electrostatic potential barrier in the region of direct grain-grain contact⁽²³⁾, the model used by *Cassia-Santos et al*⁽²⁴⁾ might be fitted the nonlinear characteristics of SrO doped TiO₂ varistors with a good agreement with the experimental data.

Table 3. Characteristics of SrO-doped TiO₂ varistors of the samples sintered at 1400°C: Activation energy (E_a), Band gap ($E_{\text{band gap}}$), Barrier height (Φ_b), Donor concentration (N_d), Density of states (N_{IS}) and Barrier width (ω).

SrO (mol%)	E_a (ev)	$E_{\text{band gap}}$	Φ_b (ev)	N_d ($\times 10^{33}$)/m ³	N_{IS} ($\times 10^{19}$)/m ²	ω ($\times 10^{-15}$)/nm
0.5	0.31	0.62	0.0004	5.45	1.36	1.24
1.0	0.42	0.84	0.00028	4.26	1.15	1,35
1.5	0.33	0.66	0.0004	5.60	1,57	1.40
2.0	0.36	0.72	0.00027	4.65	1.17	1,26

Figure 3 illustrates the impedance spectroscopy curves on the $-Z'' \times Z'$ complex measured at 325°C for the TiO₂-SrO system sintered at 1400°C. The impedance diagrams of a varistor usually takes a form of a semicircle. But the impedance diagrams of the samples doped with 0.5 (Figure 3a) present a partial semicircle, which leads to a difficulty to distinguishing the contributions of boundaries from those of grains, demonstrating a high resistance. With increasing concentration of the dopant, we notice the decrease in resistance from the doping of 1% (Figure 3b, 3c and 3d). Allowing distinguishing the boundaries of contributions from those of grains.

The best varistor behavior was presented by system containing 1% SrO, where there is a low resistance value of the grain ($R_g = 6.38 \times 10^2 \Omega$) allowing a good driving high current and high resistance value of the grain boundary ($R_{cg} = 4.57 \times 10^3 \Omega$) corresponding to the formation of the potential barrier. However, the difference between the resistance of grain and grain boundaries for these systems is still very low (an order of magnitude), which may explain the low values obtained for the coefficient of nonlinearity.

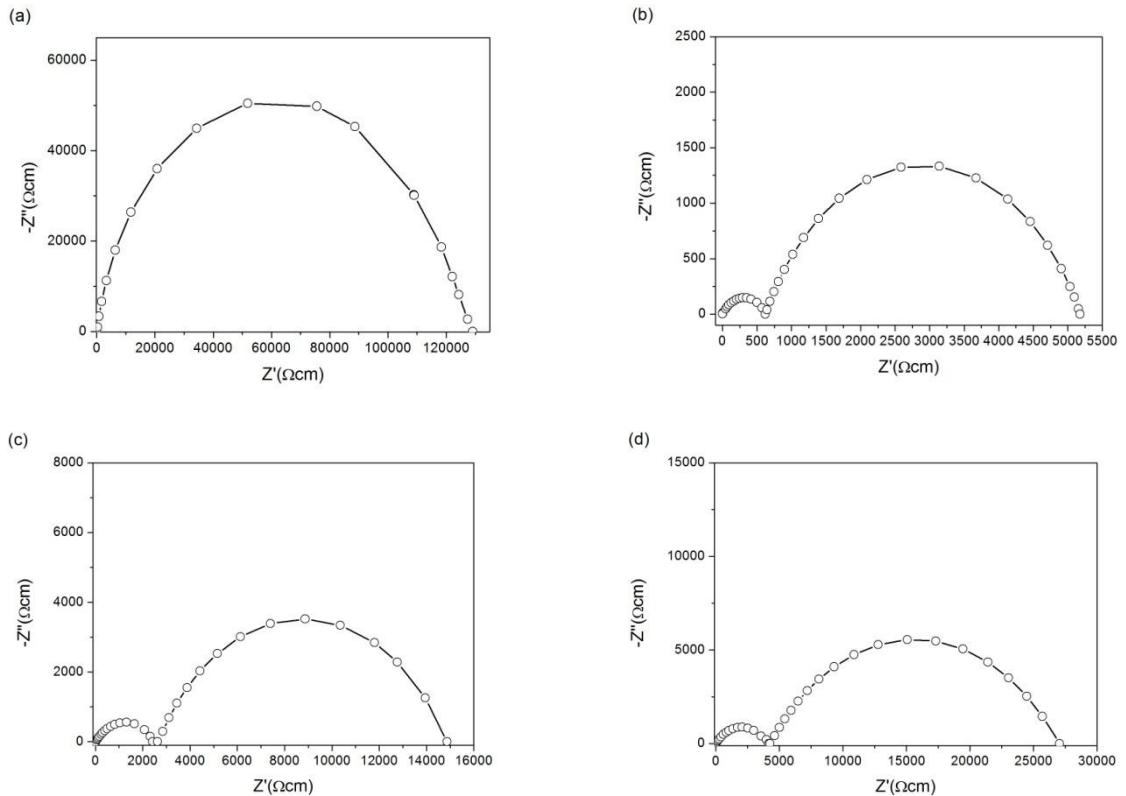


Figure 2. Nyquist diagrams for TiO_2 doped with SrO sintered at 1400°C in the following proportions: (a) 0.5%, (b) 1%, (c) 1.5% and (d) 2%.

CONCLUSIONS

Based on the results described here, it can be concluded that strontium oxide can contribute to nonlinear I - V and the potential barrier Schottky characteristics for TiO_2 varistor applications, by controlling the samples, sintering temperature, densification and dopant concentration. The grain resistivity of TiO_2 -based varistors improved with the concentration of 1% of SrO due to the distortion of the TiO_2 lattice resulting from the substitution of Ti for Sr. The results obtained in this study indicate the development of promising new binary varistor system, using SrO as the dopant for TiO_2 .

REFERENCES

(1) Mo, S.-D.; Ching, W. Electronic and optical properties of three phases of titanium dioxide: Rutile, anatase, and brookite. *Physical Review B*, v.51, n.19, p.13023, 1995.

- (2) Kavan, L.; Grätzel, M.; Gilbert, S.; Klemenz, C.; Scheel, H. Electrochemical and photoelectrochemical investigation of single-crystal anatase. *Journal of the American Chemical Society*, v.118, n.28, p. 6716–6723, 1996.
- (3) Yan, M. F.; Rhodes, W. W. Preparation and properties of TiO₂ varistors. *Applied Physics Letters*, v.40, n.6, p. 536-537, 1982.
- (4) Sousa, V.; Leite, E.; Varela, J.; Longo, E. The effect of Ta₂O₅ and Cr₂O₃ on the electrical properties of TiO₂ varistors. *Journal of the European Ceramic Society*, v.22, n.8, p.1277–1283, 2002.
- (5) Sousa, V.; Oliveira, M.; Orlandi, M.; Longo, E. Microstructure and electrical properties of (Ta, Co, Pr) doped TiO₂ based electroceramics. *Journal of Materials Science: Materials in Electronics*, v.21, n.3, p 246–251, 2010.
- (6) Wang, J. F.; Chen, H. C.; Su, W. B.; Zang, G. Z.; Wang, B.; Gao, R. W. Effects of Sr on the microstructure and electrical properties of (Co,Ta)-doped SnO₂ varistors. *Journal of Alloys and Compounds*, v. 413, n.1, p. 35–39, 2006.
- (7) Pianaro, S.; Bueno, P.; Longo, E.; Varela, J. A new SnO₂-based varistor system. *Journal of Materials Science Letters*, v.14, n.10, p. 692–694, 1995.
- (8) Fernández, H. D.; Frutos, A.; Caballero, J.; Fernández, J. F. Mott–schottky behavior of strongly pinned double schottky barriers and characterization of ceramic varistors. *Journal of Applied Physics*, v.92, n.5, p. 2890–2898, 2002.
- (9) Greuter, F.; Blatter, G. Electrical properties of grain boundaries in polycrystalline compound semiconductors. *Semiconductor Science and Technology*, v.5, n.2, p. 111, 1990.
- (10) Clarke, D. R. Varistor ceramics. *Journal of the American Ceramic Society*, v.82, n.3, p. 485–502, 1999.
- (11) Pike, G.; Seager, C. The dc voltage dependence of semiconductor grain-boundary resistance. *Journal of Applied Physics*, v.50, n.5, p. 3414–3422, 1979.
- (12) Pike, G. Semiconductor grain-boundary admittance: Theory. *Physical Review B*, v.30, n.2, p. 795, 1984.
- (13) Blatter, G.; Greuter, F. Carrier transport through grain boundaries in semiconductors. *Physical Review B*, v.33, n.6, p. 3952, 1986.
- (14) Mukae, K.; Tsuda, K.; Nagasawa, Y. Capacitance-vs-voltage characteristics of ZnO varistors. *Journal of Applied Physics*, v.50, n.6, p. 4475, 1979.
- (15) Wu, J. M.; Lal, C. H. Effect of lead oxide on niobium-doped titania varistors. *Journal of the American Ceramic Society*, v.74, n.12, p. 3112–3117, 1991.

- (16) Kröger, F. A. The chemistry of imperfect solids. North-Holland, Amsterdam, 1964.
- (17) Leite, E.; Nascimento, A.; Bueno, P.; Longo, E.; Varela, J. The influence of sintering process and atmosphere on the non-ohmic properties of SnO₂ based varistor. *Journal of Materials Science: Materials in Electronics*, v.10, n.4, p. 321–327, 1999.
- (18) Santos, M. R.; Bueno, P. R.; Longo, E.; Varela, J. A. Effect of oxidizing and reducing atmospheres on the electrical properties of dense SnO₂ -based varistors. *Journal of the European Ceramic Society*, v.21, n.2, p. 161–167, 2001.
- (19) Stucki, F.; Greuter, F. Key role of oxygen at zinc oxide varistor grain boundaries. *Applied Physics Letters*, v.57, n.5, p. 446–448, 1990.
- (20) Bueno, P.; Leite, E.; Oliveira, M.; Orlandi, M.; Longo, E. Role of oxygen at the grain boundary of metal oxide varistors: A potential barrier formation mechanism. *Applied Physics Letters*, v.79, n.1, p.48–50, 2001.
- (21) Y.-M. Chiang, D. P. Birnie, W. D. Kingery, *Physical ceramics: Principles for Ceramic Science and Engineering*, J. Wiley, 1997.
- (22) Wang, J.; Chen, F. H. C.; Su, W. B.; Zang, G. Z.; Wang, B.; Gao, R. W. Effects of Sr on the microstructure and electrical properties of (Co, Ta)-doped SnO₂ varistors *Journal of alloys and compounds*, v.413, n.1, p.35-39, 2006.
- (23) Hozer, L.; Holland, D.; Krauze, J. *Semiconductor ceramics: grain boundary effects*. New York: Ellis Horwood, 1994.
- (24) Cassia-Santos, M. R.; Bueno, P. R.; Longo, E.; Varela, J. A. *Journal of the European Ceramic Society* v. 21, p. 161, 2001.